AMERICAN SOCIETY FOR MICROBIOLOGY | Applied and Environmental Microbiology®

PHYSIOLOGY

Glycerol Phosphate Cytidylyltransferase Stereospecificity Is Key to Understanding the Distinct Stereochemical Compositions of Glycerophosphoinositol in *Bacteria* and *Archaea*

Marta V. Rodrigues, Nuno Borges, Helena Santos

Instituto de Tecnologia Química e Biológica António Xavier, Universidade Nova de Lisboa, Oeiras, Portugal

ABSTRACT Glycerophosphoinositol (GPI) is a compatible solute present in a few hyperthermophiles. Interestingly, different GPI stereoisomers accumulate in *Bacteria* and *Archaea*, and the basis for this domain-dependent specificity was investigated herein. The archaeon *Archaeoglobus fulgidus* and the bacterium *Aquifex aeolicus* were used as model organisms. The synthesis of GPI involves glycerol phosphate cytidylyltransferase (GCT), which catalyzes the production of CDP-glycerol from CTP and glycerol phosphate, and di-*myo*-inositol phosphate-phosphate synthase (DIPPS), catalyzing the formation of phosphorylated GPI from CDP-glycerol and L-*myo*-inositol 1-phosphate. DIPPS of *A. fulgidus* recognized the two CDP-glycerol stereoisomers similarly. This feature and the ability of ^{31}P nuclear magnetic resonance (NMR) to distinguish the GPI diastereomers provided a means to study the stereospecificity of GCTs. The AF1418 gene and genes aq_185 and aq_1368 are annotated as putative GCT genes in the genomes of *A. fulgidus* and *Aq. aeolicus*, respectively. The functions of these genes were determined by assaying the activity of the respective recombinant proteins: AQ1368 and AQ185 are GCTs, while AF1418 has flavin adenine dinucleotide (FAD) synthetase activity. AQ185 is absolutely specific for *sn*-glycerol 3-phosphate, while AQ1368 recognizes the two enantiomers but has a 2:1 preference for *sn*-glycerol 3-phosphate. In contrast, the partially purified *A. fulgidus* GCT uses *sn*-glycerol 1-phosphate preferentially (4:1). Significantly, the predominant GPI stereoforms found in the bacterium and the archaeon reflect the distinct stereospecificities of the respective GCTs: i.e., *A. fulgidus* accumulates predominantly *sn*-glycero-1-phospho-3-L-*myo*-inositol, while *Aq. aeolicus* accumulates *sn*-glycero-3-phospho-3-L-*myo*-inositol.

IMPORTANCE Compatible solutes of hyperthermophiles show high efficacy in thermal protection of proteins in comparison with solutes typical of mesophiles; therefore, they are potentially useful in several biotechnological applications. Glycerophosphoinositol (GPI) is synthesized from CDP-glycerol and L-*myo*-inositol 1-phosphate in a few hyperthermophiles. In this study, the molecular configuration of the GPI stereoisomers accumulated by members of the *Bacteria* and *Archaea* was established. The stereospecificity of glycerol phosphate cytidylyltransferase (GCT), the enzyme catalyzing the synthesis of CDP-glycerol, is crucial to the stereochemistry of GPI. However, the stereospecific properties of GCTs have not been investigated thus far. We devised a method to characterize GCT stereospecificity which does not require *sn*-glycerol 1-phosphate, a commercially unavailable substrate. This led us to understand the biochemical basis for the distinct GPI stereoisomer composition observed in archaea and bacteria.

Received 23 August 2016 **Accepted** 18 October 2016

Accepted manuscript posted online 21 October 2016

Citation Rodrigues MV, Borges N, Santos H. 2017. Glycerol phosphate cytidylyltransferase stereospecificity is key to understanding the distinct stereochemical compositions of glycerophosphoinositol in *Bacteria* and *Archaea*. Appl Environ Microbiol 83:e02462-16. https://doi.org/10.1128/AEM.02462-16.

Editor Shuang-Jiang Liu, Chinese Academy of Sciences

Address correspondence to Helena Santos, santos@itqb.unl.pt.

KEYWORDS Glycerol phosphate cytidylyltransferase, glycerophosphoinositol, molecular configuration, stereospecificity

Glycerophosphoinositol (GPI) is an ionic compatible solute only found thus far in hyperthermophilic bacteria and archaea of the genera *Aquifex* and *Archaeoglobus*, respectively (1). ^{31}P and ^{1}H nuclear magnetic resonance (NMR) analysis of GPI preparations derived from biomass of the natural producers indicated that different stereoisomers accumulate in archaea and bacteria (2) (Fig. 1). The two compounds generate similar ^{1}H NMR spectra but give rise to distinct ^{31}P NMR resonances: hence, they are diastereomers. However, the full characterization of the stereochemistry of the two GPI forms remained elusive.

A large number of *in vitro* studies demonstrated that negatively charged compatible solutes, highly restricted to (hyper)thermophilic marine organisms, are better protectors of proteins against heat denaturation in comparison with compatible solutes typical of mesophilic organisms, such as trehalose or glycerol (3, 4). More recently, the efficacy of one such solute, mannosylglycerate, in inhibiting protein aggregation in the cytosol of a yeast model of Parkinson's disease was also reported (5). However, the ambition for widespread utilization of these solutes in biotechnological applications is frustrated by the lack of efficient production methods. Large-scale production can be envisaged either by chemical synthesis or by introduction of the relevant biosynthetic pathways in suitable industrial hosts (synthetic biology approach). In either case, knowledge of the precise molecular structure of the natural compounds is required.

As with other polyol- or sugar-derived compatible solutes, the biosynthesis of GPI proceeds via a phosphorylated intermediate, GPI-phosphate (GPIP), which is further converted into GPI by a yet unknown phosphatase. GPIP is synthesized from CDP-glycerol and l-*myo*-inositol 1-phosphate in a reaction catalyzed by the membrane protein involved in the synthesis of di-*myo*-inositol phosphate (DIP), a canonical solute of marine hyperthermophiles. In some organisms, DIP-phosphate synthase (DIPPS), is part of a bifunctional enzyme that converts CTP and L-*myo*-inositol 1-phosphate into the phosphorylated form of di-*myo*-inositol phosphate (Fig. 2). Recently, the 3-dimensional structure of this bifunctional protein, comprising both cytosolic and transmembrane domains, has been determined (6). The soluble domain, inositol phosphate cytidylyltransferase (IPCT), catalyzes the formation of CDP-inositol from CTP and L-*myo*-inositol 1-phosphate, while the membrane domain, DIPPS, catalyzes the transfer of inositol phosphate from CDP-inositol to L-*myo*-inositol L-phosphate to yield the phosphorylated form of DIP. The latter enzyme uses exclusively L-*myo*-inositol 1-phosphate as an alcohol acceptor but is less specific for the alcohol donor as it recognizes CDP-L-*myo*-inositol, CDP-D-*myo*-inositol, and CDP-glycerol (7, 8). Consequently, phosphorylated GPI is a product of the reaction when CDP-glycerol and L-*myo*-inositol 1-phosphate are provided as the substrates (Fig. 2). All of the recombinant DIPPS enzymes characterized thus far are able to synthesize DIP and GPI (8). However, the solute GPI has been found only in species of the genera *Archaeoglobus* and *Aquifex* (1).

We determined the stereochemistry of the L-*myo*-inositol 1-phosphate moiety in GPI by ^{13}C isotopic labeling and NMR analysis to prove that the phosphate group is linked at position 3 of *myo*-inositol (the numbering of the inositol atoms is based on the L-configuration according to the "relaxation of lowest-locant rule" as recommended by the Nomenclature Committee of the International Union of Biochemistry), regardless of the bacterial or archaeal origin of the enzyme (8). However, the stereochemistry of the glycerol moiety has not been determined.

CDP-glycerol is synthesized by the action of glycerol phosphate cytidylyltransferase (GCT) from CTP and glycerol phosphate. All GCTs characterized thus far have a bacterial origin and can use *sn*-glycerol 3-phosphate to form CDP-3-glycerol, a precursor for the synthesis of poly(glycerol phosphate), which is a major component of the cell wall teichoic acids of Gram-positive bacteria (9). The observation that cell wall teichoic acids

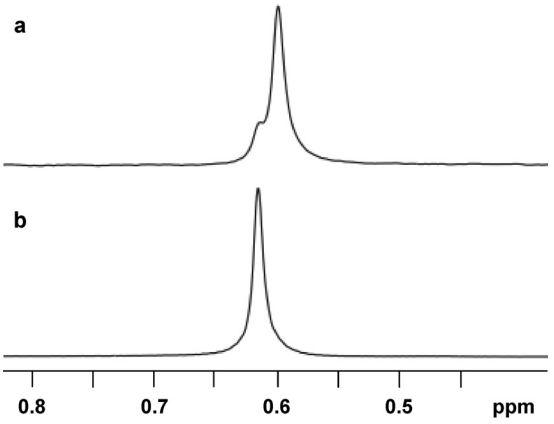

FIG 1 ^{31}P NMR of GPI accumulated by *Archaeoglobus fulgidus* (a) and *Aquifex aeolicus* (b). The GPI preparations were obtained from cell biomass through ethanolic extraction (adapted from reference 2).

of *Bacillus subtilis* are essential for cell viability drew attention to this promising antimicrobial drug target. Prompted by this medical interest, several GCTs from *Bacillus subtilis*, *Staphylococcus aureus*, *Listeria monocytogenes*, and *Enterococcus faecalis* have been biochemically and structurally characterized (10–17). Oddly, in contrast with the

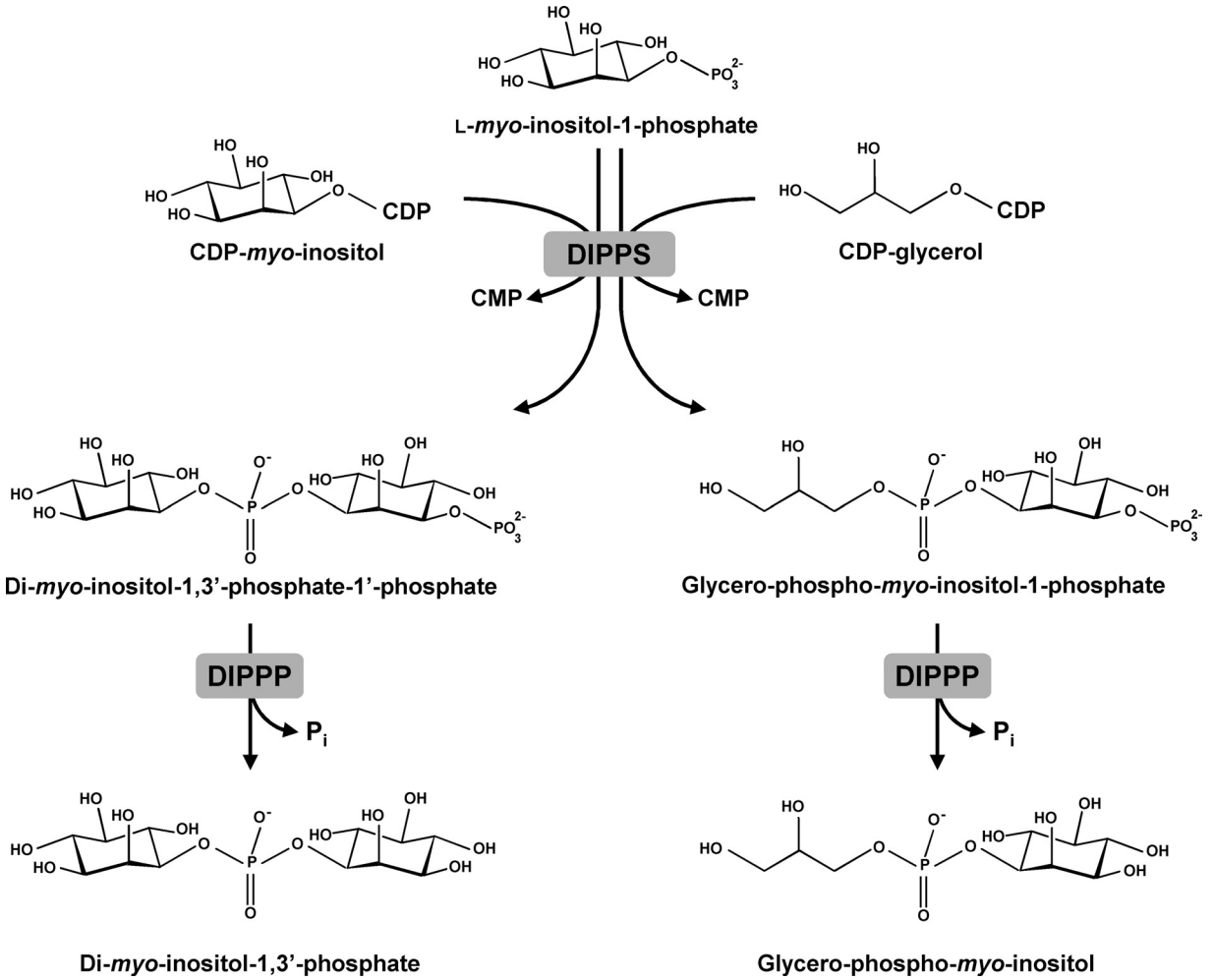

FIG 2 Pathways for the synthesis of di-*myo*-inositol phosphate (DIP) and glycerophosphoinositol (GPI). The DIP-phosphate synthase (DIPPS) catalyzes the condensation of L-*myo*-inositol 1-phosphate with CDP-inositol or with CDP-glycerol, producing DIP-phosphate or GPI-phosphate, respectively. Subsequently, phosphorylated intermediates are converted into DIP or GPI by unknown DIPP phosphatase(s) (DIPPP).

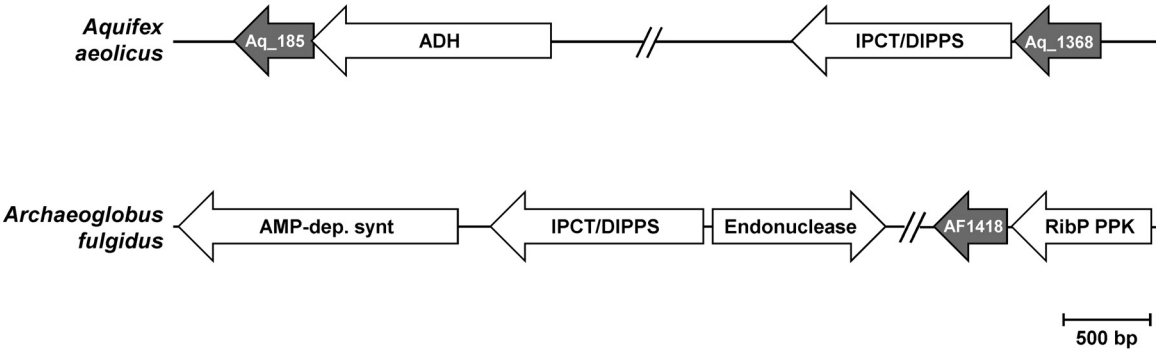

FIG 3 Schematic organization of the genes encoding the enzymes implicated in the synthesis of glycerophosphoinositol (GPI), CDP-glycerol, or FAD in *Aquifex aeolicus* and *Archaeoglobus fulgidus*. Aq_185 and Aq_1368, genes encoding glycerol phosphate cytidylyltransferases; AF1418, gene encoding an FAD synthetase; ADH, aldehyde dehydrogenase; IPCT, inositol phosphate cytidylyltransferase; DIPPS, di-*myo*-inositol phosphate-phosphate synthase, which also catalyzes the synthesis of GPI-phosphate; AMP-dep. synt, AMP-dependent synthetase; and RibP PPK, ribose phosphate pyrophosphokinase.

great research effort directed to the determination of 3-dimensional structures and catalytic mechanisms, there is no information on the specificity of these enzymes for the enantiomers of glycerol phosphate.

In this work, the configuration of the GPI stereoisomers synthesized in members of the *Bacteria* and *Archaea* was identified and the biochemical basis for the domain-dependent specificity was investigated. To this end, we devised a method to study the stereospecificity of the GCTs, which does not require *sn*-glycerol 1-phosphate, a commercially unavailable substrate. Moreover, genes aq_1368, aq_185 and AF1418 were functionally characterized after heterologous expression in *Escherichia coli*.

RESULTS

Functional studies. The archaeon *Archaeoglobus fulgidus* and the bacterium *Aquifex aeolicus* accumulate different diastereomers of GPI (Fig. 1). As previously established by ^{13}C-specific isotopic labeling and NMR analysis, the inositol moiety has the same stereochemical configuration in the two natural diastereomers (2, 8); hence, the glycerol moieties must have distinct configurations.

Glycerol phosphate cytidylyltransferases (GCTs) are the key enzymes in the synthesis of CDP-glycerol, one of the precursors of GPI (7) (Fig. 2). Genomic analysis revealed the presence of one gene in *A. fulgidus* (AF1418) and two genes in *Aq. aeolicus* (aq_185 and aq_1368) coding for putative GCTs (Fig. 3). These genes were cloned and expressed in *Escherichia coli*, and the activity of the encoded proteins was investigated in cell extracts. GCT activity was detected in cells producing either AQ185 or AQ1368 (Fig. 4), but no such activity was detected for the gene product of *A. fulgidus* (AF1418). Recently, the annotation of the *A. fulgidus* genome was revised, and the AF1418 gene was assigned to putative flavin adenine dinucleotide synthetase (FADS). We confirmed that cell extracts of *E. coli* harboring the synthetic AF1418 gene did activate flavin mononucleotide (FMN) with ATP, yielding FAD (Fig. 4). Pure recombinant AQ1368 and AQ185 were also assayed for FADS activity: very weak FAD signals were detected only for the latter enzyme. In summary, we found that AQ1368 and AQ185 are GCTs, while AF1418 is an FADS. BLAST searches were carried out in the genome of *A. fulgidus*, using the sequences of *Aq. aeolicus* GCTs (AQ1368 and AQ185) as the query, but no good candidate to encode a GCT was found. However, we confirmed the presence of GCT activity in cell extracts of *A. fulgidus* and decided to perform subsequent characterization studies with a partially purified preparation of the native enzyme, herein designated "partially purified *A. fulgidus* GCT."

Approach to study the stereospecificity of GCTs. We designed a procedure to determine the stereospecificity of CGTs for *sn*-glycerol 3-phosphate and *sn*-glycerol 1-phosphate, which does not require pure *sn*-glycerol 1-phosphate, a compound not available commercially. The protocol comprises two steps (Fig. 5). In the first one,

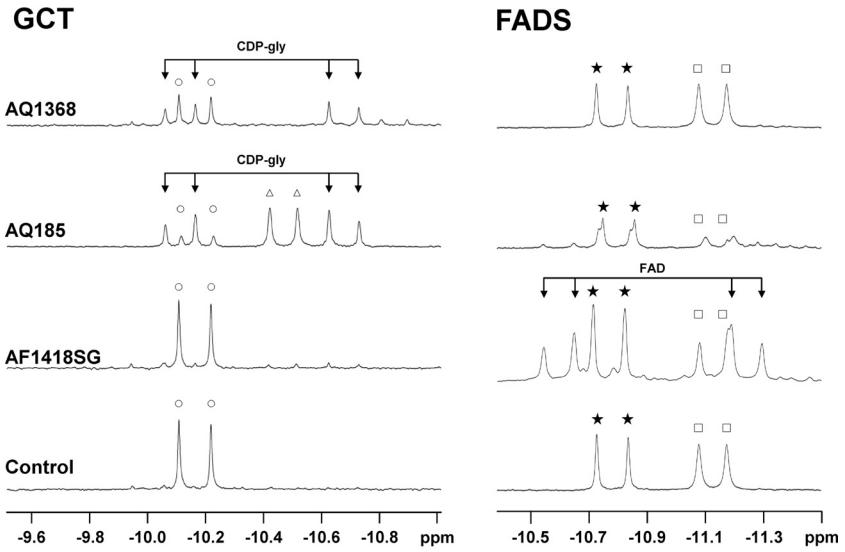

FIG 4 Assays for glycerol phosphate cytidylyltransferase (left panel) and FAD synthetase (right panel) activities. The traces are sections of ^{31}P NMR spectra of reaction mixtures after incubation at 80°C of the relevant substrates and cofactors with cell extracts of *E. coli* harboring pET19b (control), pET19b:AF_1418SG, pET19b:aq_185, and pET19b:aq_1368. The reaction mixture for detection of GCT activity contained the following: 4 mM CTP, 4 mM *rac*-glycerol phosphate, and 10 mM $MgCl_2$ in 50 mM Tris-HCl buffer (pH 8.6). The reaction mixture for detection of FADS activity contained the following: 10 mM ATP, 5 mM FMN, 15 mM DTT, and 10 mM $MgCl_2$ in 50 mM Tris-HCl buffer (pH 8.6). FAD, flavin adenine dinucleotide; CDP-gly, CDP-glycerol. Resonance symbols: ○, CTP; △, CDP; ⋆, ATP; □, ADP.

CDP-glycerol is produced by the target GCT from the substrates CTP and *rac*-glycerol phosphate. NMR cannot distinguish the stereoisomers of CDP-glycerol; hence, a second step is needed to produce diastereomeric products, which can be quantified by ^{31}P NMR. We knew from previous work that archaea and bacteria that accumulate di-*myo*-inositol phosphate are able to synthesize GPI from CDP-glycerol and L-*myo*-inositol 1-phosphate (8). This results from a side reaction catalyzed by DIPPS, an enzyme that recognizes CDP-glycerol in addition to CDP-inositol, the preferred substrate. Therefore, cell extracts of *A. fulgidus* were selected to perform the conversion of CDP-glycerol into GPI. Additionally, we probed whether the relevant synthase, the transmembrane domain of IPCT/DIPPS, used the two stereoisomers of CDP-glycerol to a similar extent. For this purpose, cell extracts of *A. fulgidus* were incubated with a racemic mixture of CDP-glycerol (purchased from Sigma) and L-*myo*-inositol 1-phosphate. After 1 h of incubation, the proportion of the two forms of GPI was evaluated by ^{31}P NMR. The average ratio from four independent experiments was 1:1.2, denoting only a slight preference for *sn*-glycerol 1-phosphate (see Fig. S1 in the supplemental material).

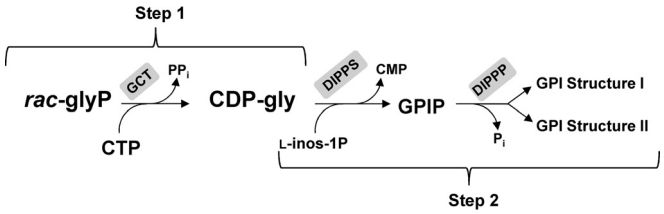

FIG 5 Scheme representing the method used to characterize the stereospecificity of GCTs. Step 1 represents production of CDP-glycerol from *rac*-glycerol phosphate by the target glycerol phosphate cytidylyltransferase. Step 2 represents conversion of CDP-glycerol produced in step 1 into GPI via de action of the DIPP synthase and phosphatase activities present in the *A. fulgidus* cell extract provided. Finally, ^{31}P NMR analysis of the reaction products enables the determination of the stereoforms of GPI produced and, indirectly, the proportions of *sn*-glycerol 3-phosphate and *sn*-glycerol 1-phosphate used by the GCT enzyme. GCT, glycerol phosphate cytidylyltransferase; DIPPS, di-*myo*-inositol phosphate-phosphate synthase; DIPPP, DIPP phosphatase; *rac*-glyP, *rac*-glycerol phosphate; L-inos-1P, L-*myo*-inositol 1-phosphate.

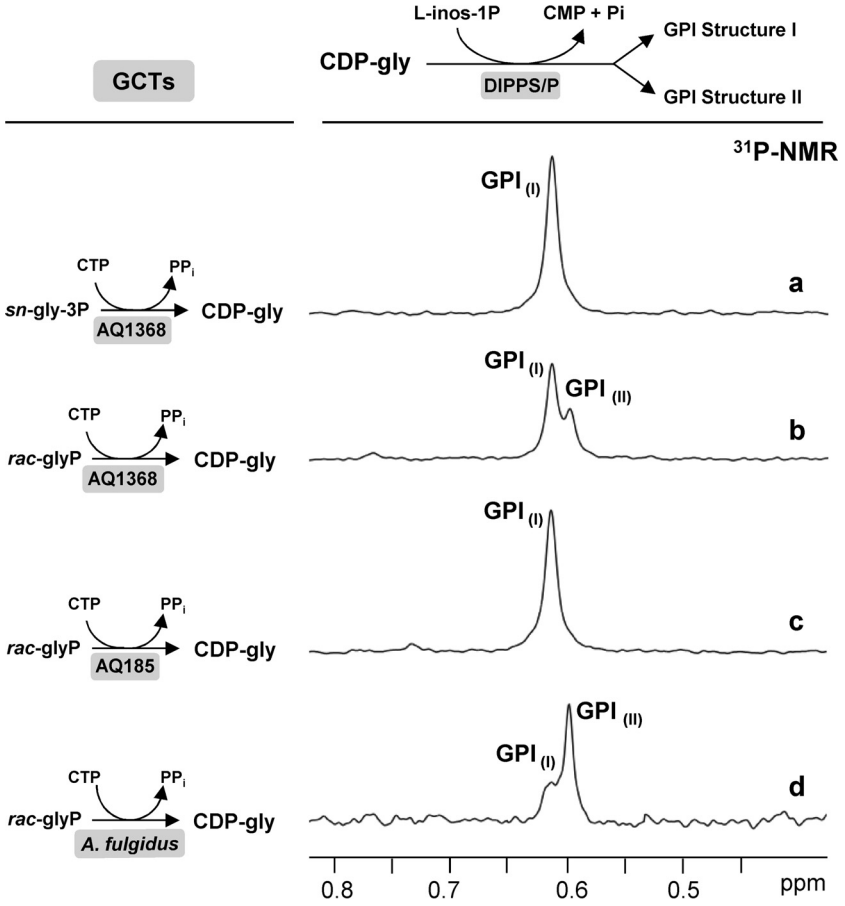

FIG 6 Final step in the characterization of GCT stereospecific properties. Traces show the ^{31}P NMR resonances due to the GPI formed by the auxiliary enzymes DIPP synthase/phosphatase in cell extracts of *Archaeoglobus fulgidus* using CDP-glycerol produced by the GCTs examined in this study (indicated on the left-hand side). (a and b) recombinant AQ1368, (c) recombinant AQ185, and (d) GCT activity partially purified from a cell extract of *Archaeoglobus fulgidus*. The stereospecificity of each GCT for *sn*-glycerol 3-phosphate and *sn*-glycerol 1-phosphate was determined from the areas of the resonances attributed to GPI structure I and GPI structure II in the ^{31}P NMR spectra of the final reaction mixtures.

Identification of the stereochemical configuration of GPI in *Aq. aeolicus* and *A. fulgidus*. To determine the configuration of the glycerol moiety in GPIs, CDP-3-glycerol was produced by using *Aq. aeolicus* GCT (AQ1368) and the substrates *sn*-glycerol 3-phosphate and CTP. Then CDP-3-glycerol was incubated with L-*myo*-inositol 1-phosphate and a cell extract of *A. fulgidus*, producing *sn*-glycero-3-phospho-3-L-*myo*-inositol (Fig. 6a). The phosphodiester group in this compound resonates at 0.62 ppm and coincides with the GPI detected in the bacterial species (Fig. 1). When the reaction was carried out with *rac*-glycerol phosphate instead of *sn*-glycerol 3-phosphate, two resonances (at 0.62 and 0.60 ppm) were observed in the ^{31}P NMR spectrum of the reaction products (Fig. 6b). To exclude the possibility that these signals are due to the phosphorylated form of GPI, the reaction mixture was incubated with alkaline phosphatase, and no alteration of these resonances was observed (data not shown). Therefore the resonance at 0.62 ppm is due to *sn*-glycerol 3-phospho-3-L-*myo*-inositol, and the signal at 0.60 ppm is assigned to *sn*-glycero-1-phospho-3-L-*myo*-inositol. We conclude that the glycerol moiety of GPI encountered in the solute pool of *Aq. aeolicus* derives from *sn*-glycerol 3-phosphate, while the major GPI form in *A. fulgidus* derives from *sn*-glycerol 1-phosphate. The molecular structures of GPIs accumulated by *A. fulgidus* and *Aq. aeolicus* are shown in Fig. 7.

Stereospecificity of the GCTs from *Aq. aeolicus* and *A. fulgidus*. The strategy described above, which used a racemic mixture of glycerol phosphate, was followed to

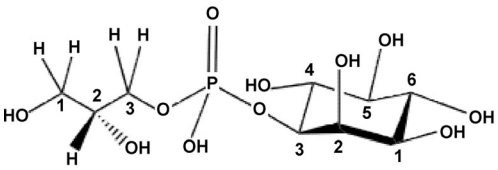

Structure I

***sn*-glycero-3-phospho-3-L-*myo*-inositol**

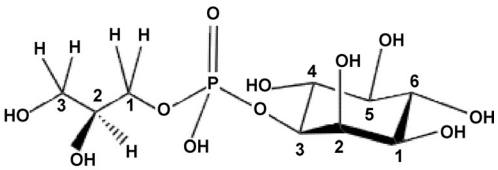

Structure II

***sn*-glycero-1-phospho-3-L-*myo*-inositol**

FIG 7 The structures of two stereoisomers of GPI. Structure I is the sole form present in *Aquifex* spp. and a minor component in the archaeon *Archaeoglobus fulgidus*, which accumulates primarily the form represented by structure II. The carbon atoms of glycerol are numbered stereospecifically: i.e., the carbon atom that appears on the top of the Fischer projection that has the hydroxyl group at carbon 2 pointing to the left is designated C-1 (26).

characterize the stereospecificity of recombinant *Aq. aeolicus* GCT (AQ185) and *Aq. aeolicus* GCT (AQ1368), as well as the partially purified *A. fulgidus* GCT. CDP-glycerol produced with *Aq. aeolicus* GCT (AQ1368) generated two forms of GPI (resonances at 0.60 and 0.62 ppm) in the subsequent step catalyzed by the auxiliary DIPPS present in *A. fulgidus* cell extract (Fig. 6b). Quantification of the respective signals shows that the *Aq. aeolicus* GCT (AQ1368) produces 66% CDP-3-glycerol and 34% CDP-1-glycerol. Therefore, the preference of GCT *Aq. aeolicus* (AQ1368) for *sn*-glycerol 3-phosphate over *sn*-glycerol 1-phosphate is approximately 2-fold. In contrast, GCT *Aq. aeolicus* (AQ185) has absolute specificity for *sn*-glycerol 3-phosphate since a single GPI product was observed (resonance at 0.62 ppm) (Fig. 6c).

The GCT activity of *A. fulgidus* recognized both enantiomers of glycerol phosphate, with a clear preference for *sn*-glycerol 1-phosphate. The proportion of *sn*-glycerol 1-phosphate incorporated is approximately 4 times higher than that of *sn*-glycerol 3-phosphate (Fig. 6d).

DISCUSSION

The genomes of *A. fulgidus* and *Aq. aeolicus* comprise one (AF1418) and two (aq_185 and aq_1368) genes encoding putative GCTs, respectively. Expression of these genes in *E. coli* confirmed that the gene products of *Aq. aeolicus* (AQ185 and AQ1368) catalyze the synthesis of CDP-glycerol from CTP and glycerol phosphate. AQ1368 is located immediately upstream of the IPCT/DIPPS gene, while the gene coding for AQ185 is located elsewhere in the genome. Therefore, we propose that AQ1368 is the GCT implicated in the synthesis of CDP-glycerol, a precursor for the synthesis of GPI by the DIPPS enzyme of *Aq. aeolicus*. AQ185 is also able to catalyze CDP-glycerol formation, but its physiological role is most likely unrelated to GPI synthesis. Interestingly, the AF1418 protein, earlier annotated as a putative GCT, showed no such activity; instead it catalyzed the synthesis of FAD from ATP and FMN. Moreover, BLAST searches with known GCTs revealed no hit in the *A. fulgidus* genome, despite the observation of GCT activity in cell extracts of this archaeon. This activity must be encoded by a gene with poor sequence similarity to known GCT genes; hence the identification of the gene encoding this novel archaeal GCT looks like an interesting challenge. To date, no GCT has been assigned in the domain *Archaea*.

The enzymes GCTs and FADSs are nucleotidyltransferases that catalyze related reactions: formation of CDP-glycerol with release of PP_i from the cytidylation of glycerol phosphate with CTP or formation of FAD with release of PP_i from the adenylation of FMN with ATP. In bacteria, FADS is the N-terminal domain of a bifunctional protein in which the C-terminal domain is responsible for the phosphorylation of riboflavin, while in eukaryotes, the two proteins are encoded by separate genes. Bacterial and eukaryal FADSs show very little sequence similarity (18, 19); accordingly, they are classified into distinct protein families: the FADS family (PF06574), and the phosphoadenosine phosphosulfate reductase family (PF01507), respectively (http://pfam.xfam.org/). On the other hand, the two known archaeal FADS proteins from *A. fulgidus* and *Methanocal-*

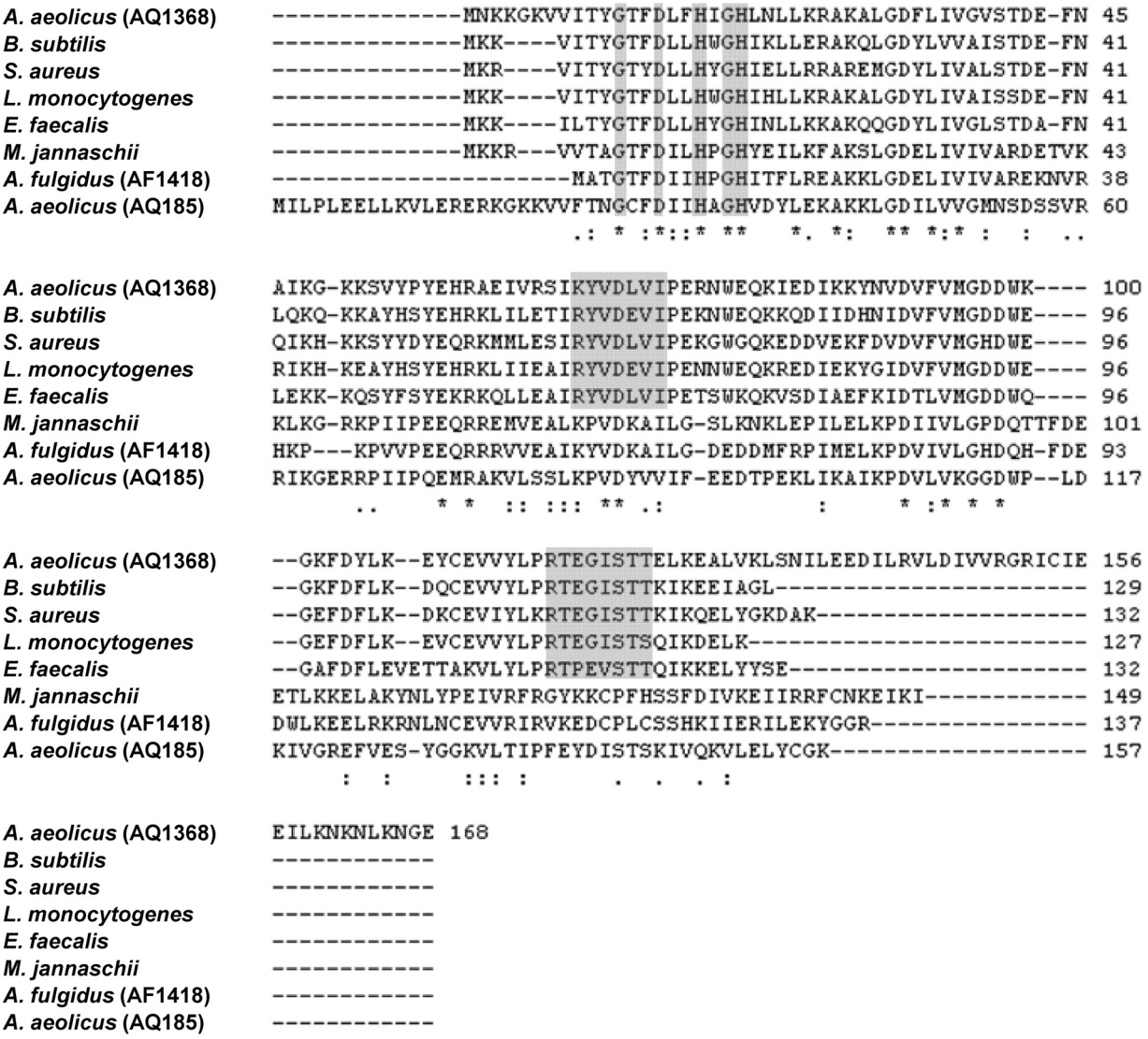

FIG 8 Multiple-sequence alignment of the amino acid sequences of the glycerol phosphate cytidylyltransferases of *Aquifex aeolicus* (AQ185 and AQ1368), *Bacillus subtilis*, *Staphylococcus aureus*, *Listeria monocytogenes*, and *Enterococcus faecalis* and of the FAD synthetase of *Archaeoglobus fulgidus* (AF1418), and *Methanocaldococcus jannaschii* (27). The alignment was generated with ClustalW2 (https://www.ebi.ac.uk/Tools/msa/clustalw2/). Gray boxes highlight conserved motifs.

dococcus jannaschii belong to yet a different protein family, the cytidylyltransferase family (PF01467), which also comprises all GCTs characterized thus far.

Three conserved motifs have been assigned in GCTs: the H*X*GH sequence, comprising two histidine residues involved in catalysis, is present in the GCTs of *Bacillus subtilis*, *Staphylococcus aureus*, *Listeria monocytogenes*, *Enterococcus faecalis*, and *Aq. aeolicus* (AQ1368 and AQ185) (Fig. 8). The two other conserved motifs of GCTs are RYVDEVI and, most importantly, RTXGISTT, which is considered to be a signature of this group of proteins (10, 11, 15). It is curious that the two GCTs of *Aq. aeolicus* are part of different clusters (Fig. 9): AQ1368 falls in the cluster comprising known bacterial GCTs, while the other is found in the archaeal FADS cluster, despite its poor activity for the synthesis of FAD. In brief, AQ185 shows a major GCT activity without possessing the so-called signature motif of GCTs.

To our knowledge, only four bacterial GCTs have been characterized thus far (10, 12, 13, 16, 17, 20, 21), but their stereospecific properties have not been reported. The strategy designed here to study the GCT stereospecific properties (Fig. 5) led to the conclusion that the recombinant *Aq. aeolicus* GCT (AQ1368) and *Aq. aeolicus* GCT

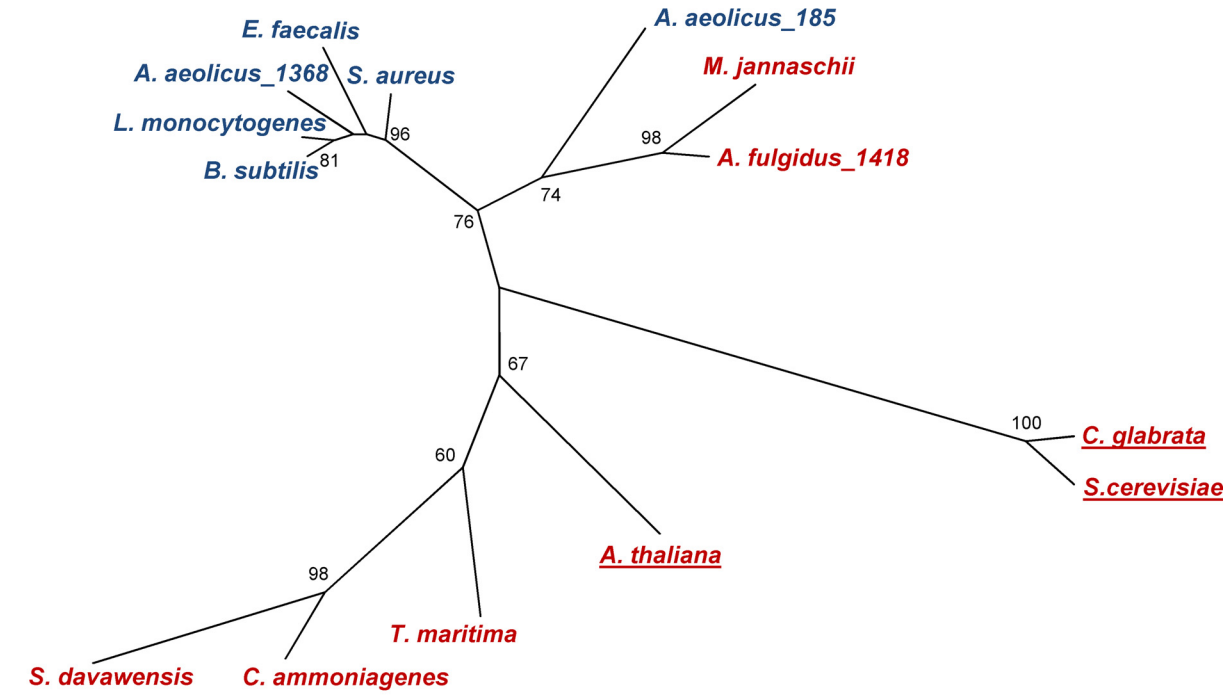

FIG 9 Phylogenetic tree based on amino acid sequences of glycerol phosphate cytidylyltransferases (GCTs), bifunctional riboflavin kinase/FMN adenylyltransferases (FADS/RibFKs), and flavin adenine dinucleotide synthetases (FADSs), whose functions have been proven. Only the FADS domain of the bifunctional FADS/RibFKs was used for this analysis. MEGA6 software (28) used for sequence alignment and to draw the tree. Bootstrap values were calculated from 1,000 replicates. Only bootstrap values greater than or equal to 60 are shown. The scale bar represents the branch lengths measured in the number of substitutions per site. Organisms harboring the GCT and FADS proteins are indicated in blue and red, respectively. Underlined names refer to eukaryotic organisms. GenPept accession numbers for the FADS and GCT proteins are provided in parentheses for the following organisms: for bifunctional RibFK/FADS, *Corynebacterium ammoniagenes* (Q59263.1), *Thermotoga maritima* (1T6Y), and *Streptomyces davawensis* (ABN55909.1); for FADS, *Arabidopsis thaliana* (Q9FMW8.1), *Methanocaldococcus jannaschii* (WP_010870692), and *Archaeoglobus fulgidus* AF1418 (WP_048064389.1); and for GCT, *Aquifex aeolicus* AQ1368 (NP_213944.1), *Candida glabrata* (3G5A), *Saccharomyces cerevisiae* (AAA65730.1), *Bacillus subtilis* (1COZ), *Aquifex aeolicus* AQ185 (NP_213132.1), *Staphylococcus aureus* (AAB51063.1), *Listeria monocytogenes* (WP_003727003), and *Enterococcus faecalis* (EEI58902).

(AQ185) showed a high preference (around 66%) and absolute preference for *sn*-glycerol 3-phosphate, respectively. In contrast, the *A. fulgidus* GCT exhibited a strong preference for *sn*-glycerol 1-phosphate (around 80%). Significantly, the bacterium *Aq. aeolicus* accumulates exclusively *sn*-glycero-3-phospho-3-L-*myo*-inositol, whereas the archaeon *A. fulgidus* accumulates mainly *sn*-glycero-1-phospho-3-L-*myo*-inositol, with small amounts of *sn*-glycero-1-phospho-3-L-*myo*-inositol (Fig. 1). Therefore, the ratio of the two GPI stereoforms in the solute pool of *A. fulgidus* appears to reflect perfectly the preference of its GCT for *sn*-glycerol 1-phosphate over *sn*-glycerol 3-phosphate. However, the issue of substrate availability should not be ignored in this discussion.

A. fulgidus possesses two enzymes involved in the synthesis of *sn*-glycerol 3-phosphate (WP_010878372.1 and WP_010878825.1) and one enzyme for the synthesis of *sn*-glycerol 1-phosphate (WP_010879170.1). Unfortunately, the lack of data on the relative intracellular concentrations of *sn*-glycerol 1-phosphate and *sn*-glycerol 3-phosphate in *A. fulgidus*, or any other archaeon, precludes further elaboration on the relevance of substrate availability. On the other hand, it is clear that the exclusive accumulation of one of the stereoforms of GPI (structure I) in *Aq. aeolicus* is determined ultimately by substrate availability. In fact, this bacterium does not possess *sn*-glycerol 1-phosphate dehydrogenase or any other enzyme involved in the synthesis of *sn*-glycerol 1-phosphate; hence, *sn*-glycerol 3-phosphate is the sole enantiomer available to be processed by GCTs in *Aq. aeolicus*.

Different enantiomers of glycerol phosphate are used in the glycerophosphate backbones of membrane phospholipids of bacteria and archaea. While *sn*-glycerol 1-phosphate is found in the phospholipids of members of the domain *Archaea*, *sn*-glycerol 3-phosphate is found in phospholipids of *Bacteria* and *Eukarya* (22). In fact, the presence of different enantiomers of glycerol phosphate in the membrane phospholipids of *Bacteria* and *Archaea* is the most distinctive feature of the two domains, and until now, no exceptions to this rule had been found (23). This feature seems to match up the occurrence of different stereoforms of GPI in archaea and bacteria together with the dissimilar stereospecific properties of the archaeal and bacterial GCTs studied in this work.

In conclusion, the molecular configuration of the GPI forms accumulated in the archaeon *A. fulgidus* and in the bacterium *Aq. aeolicus* were established herein. Moreover, we proved that the bacterial GCTs use primarily *sn*-glycerol 3-phosphate, while the GCT from *A. fulgidus* has a strong preference for *sn*-glycerol 1-phosphate. Therefore, the predominance of *sn*-glycero-1-phospho-3-L-*myo*-inositol in the archaeon and of *sn*-glycero-3-phospho-3-L-*myo*-inositol in the bacterium fits with the stereoisomer preference of the respective GCTs. This is the first report on the stereospecific properties of any GCT.

MATERIALS AND METHODS

Materials. Glycerol phosphate (racemic mixture of *sn*-glycerol 3-phosphate and *sn*-glycerol 1-phosphate), *sn*-glycerol 3-phosphate, CTP, CDP-glycerol (racemic mixture of CDP-1-glycerol and CDP-3-glycerol), ATP, NAD^+, flavin mononucleotide (FMN), flavin adenine dinucleotide (FAD), and 1,4-dithiothreitol (DTT), were purchased from Sigma-Aldrich (St. Louis, MO).

Growth of *A. fulgidus* and preparation of cell extracts. *A. fulgidus* strain 7324 (Deutsche Sammlung von Mikroorganismen und Zellkulturen, Braunschweig, Germany) was grown at 83°C in 2-liter static vessels with a gas phase composed of N_2 in the medium described previously (7). Cell growth was assessed by measuring the optical density at 600 nm (OD_{600}). Cells were harvested by centrifugation (8,671 × *g*, 20°C, 10 min) during the late exponential growth phase (maximal OD_{600} of 0.27) and washed with a solution of 3% (wt/vol) NaCl. The cell pellet was suspended in 10 mM Tris-HCl (pH 7.6) containing 5 mM $MgCl_2$, and the cells were disrupted in a French press. The cell debris was removed by centrifugation (15,557 × *g*, 4°C, 45 min). For the enzymatic assays, the supernatant was applied to a PD-10 column (GE Healthcare) previously equilibrated with 50 mM Tris-HCl (pH 7.6) to remove low-molecular-mass compounds. For the partial purification of the native *A. fulgidus* GCT, the supernatant was dialyzed against 50 mM Tris-HCl (pH 7.6) using a membrane with a 3.5-kDa-molecular-mass cutoff. The protein content was estimated by the Bradford method (24).

Partial purification of the native *A. fulgidus* GCT. The cell extracts (approximately 132 mg of total protein) were applied to a Resource Q column (GE Healthcare) equilibrated with 50 mM Tris-HCl (pH 7.6) and eluted with a linear gradient of NaCl (from 0 to 1 M) of the same buffer. GCT activity was detected in the flowthrough and in the fractions eluted between 0.25 and 0.5 M NaCl. The eluted fractions were pooled, dialyzed against 50 mM Tris-HCl (pH 7.6), and concentrated using a Centricon filter (Millipore).

Cloning, expression, and purification of putative GCTs. The genes aq_185 (NP_213132.1) and aq_1368 (NP_213944.1) from *Aq. aeolicus* and the AF1418 gene (NP_070247.1) from *A. fulgidus* are annotated in their respective genomes as GCT-encoding genes. Chromosomal DNAs from *Aq. aeolicus* and *A. fulgidus* were isolated as described by Rodrigues et al. (8). The two genes from *Aq. aeolicus* were amplified by PCR using *Taq* DNA polymerase (Bioline) and cloned into pET19b following standard protocols (25). The correct sequences of the cloned genes were confirmed (Stab-Vida, Portugal). *E. coli* BL21(DE3) cells, containing the constructs, were grown at 37°C in LB medium with ampicillin (100 μg/μl) until an OD_{600} of 0.6 to 0.7 and induced with 0.5 mM isopropyl β-D-1-thiogalactopyranoside (IPTG) for 4 h. The cells were harvested, suspended in 10 mM Tris-HCl (pH 7.6) containing 5 mM $MgCl_2$, and disrupted in a French press; cell debris was removed as described above. The histidine-tagged recombinant proteins were purified from cell extracts (approximately 112 and 102 mg of total protein for AQ1368 and AQ185, respectively) by using a HisTrap HP column (GE Healthcare). Elution was carried out with 0.5 M imidazole. The enzymes were judged as pure by SDS-PAGE (data not shown). The gene AF1418 from *A. fulgidus* was cloned into pET19b, pET52b, and pTRC99a. The gene sequences of the constructs were confirmed by DNA sequencing (Stab-Vida, Portugal). These constructs were transformed into *E. coli* BL21(DE3) and Rosetta(DE3), and these cells were grown at different temperatures (18, 30, and 37°C) and IPTG concentrations (0, 0.5, and 1 mM). All recombinant proteins of AF1418 were expressed in inclusion bodies. The synthetic *E. coli* optimized gene was purchased from Geneart (Life Technologies). The synthetic gene (AF1418SG) was cloned into pET19b and transformed into *E. coli* BL21(DE3). Cells were grown at 37°C in LB medium with ampicillin (100 μg/μl) until an OD_{600} of 0.7 to 0.8, and protein expression was induced with 0.5 mM IPTG for 5 h. Several attempts to purify AF1418SG were performed, but the purification yield was very poor. Therefore, the characterization of the enzyme activity was performed in cell extracts of *E. coli* BL21(DE).

Production and purification of L-*myo*-inositol 1-phosphate. L-*myo*-Inositol 1-phosphate was produced and purified as previously described (7, 8). Briefly, the recombinant L-*myo*-inositol 1-phosphate synthase from *A. fulgidus* was incubated with 20 mM Tris-HCl (pH 7.6), 10 mM $MgCl_2$, 10 mM glucose-6-phosphate, and 5 mM NAD^+ for 1 h at 85°C. The synthesized L-*myo*-inositol 1-phosphate was applied to a QAE-Sephadex A-25 column, equilibrated with 5 mM $NaHCO_3$ (pH 9.8). The elution was carried out with a linear gradient of 5 mM to 1 M $NaHCO_3$ (pH 9.8). The eluted fractions were analyzed by ^{1}H NMR. The fractions containing L-*myo*-inositol 1-phosphate were pooled and desalted in the HCl-activated Dowex 50W-X8 resin. The elution was carried out with distilled H_2O. Subsequently the fractions were pooled, and the pH was adjusted to 5.3. The sample was lyophilized, and the L-*myo*-inositol 1-phosphate was quantified by ^{1}H NMR.

Production of CDP-glycerol using the GCTs from *A. fulgidus* and *Aq. aeolicus*. Partially purified GCT from *A. fulgidus* (approximately 2 mg of total protein) was incubated at 80°C in 50 mM Tris-HCl (pH 8.6) containing 10 mM $MgCl_2$ with 4 mM CTP and 4 mM *rac*-glycerol phosphate (or 4 mM *sn*-glycerol 3-phosphate) (total volume of 400 μl). The reactions were stopped after 45 min by the addition of 15 mM EDTA (pH 8.0). After centrifugation (16,100 $\times$ *g*, 15 min, 4°C), the supernatants were lyophilized. The residues were suspended in water and treated with alkaline phosphatase for 45 min at 37°C to dephosphorylate residual substrates. The alkaline phosphatase was inactivated at 80°C for 15 min. The CDP-glycerol was quantified by ^{31}P NMR. For the production of CDP-glycerol with the *Aq. aeolicus* enzyme, the reaction mixtures were incubated at 85°C in 50 mM Tris-HCl (pH 8.6) containing 10 mM $MgCl_2$ in the presence of 10 mM CTP and 10 mM *rac*-glycerol phosphate or 10 mM *sn*-glycerol 3-phosphate. Reactions were started by the addition of 150 μg of AQ185 or 50 μg of AQ1368. After 1 h of incubation, the mixtures were centrifuged (16,100 $\times$ *g*, 15 min, 4°C), and the supernatant was lyophilized and treated with alkaline phosphatase as described above. The CDP-glycerol produced was quantified by ^{31}P NMR.

Analysis of the stereoform composition of CDP-glycerol. CDP-glycerol produced with GCT of *A. fulgidus* or *Aq. aeolicus* was incubated at 80°C for 1 h with cell extracts of *A. fulgidus*. The reaction mixture (total volume of 800 μl), contained cell extract (around 18 mg of total protein), 50 mM Tris-HCl (pH 8.6), 10 mM $MgCl_2$, 3.5 mM L-*myo*-inositol 1-phosphate, and 0.4 mM CDP-glycerol. CDP-glycerol was converted into GPI due to the consecutive actions of DIPPS and DIPP phosphatase present in *A. fulgidus* cell extract (Fig. 2). After lyophilizing, the residue was suspended in 500 μl of ^2H_2O with 30 mM EDTA (pH 8), and reaction products were analyzed by ^{31}P NMR. The GPI diastereomers' resonances are partially overlapped, hampering direct integration. Therefore, deconvolution of the relevant spectral region was performed by fitting the sum of Lorentzian and Gaussian functions using Matlab V7.1 (Math Works, Natick, MA).

Enzyme assays. The GCT and FAD synthetase activities were determined in the AF1418SG, AQ185, and AQ1368 preparations. For the detection of GCT activity, these enzymes were incubated with 50 mM Tris-HCl (pH 8.6), 10 mM $MgCl_2$, 4 mM CTP, and 4 mM glycerol phosphate for 45 min at 80°C. The FAD synthetase activity was evaluated in reaction mixtures containing 50 mM Tris-HCl (pH 8.6), 10 mM $MgCl_2$, 10 mM ATP, 5 mM FMN, and 15 mM DTT for 45 min at 80°C. The reaction products (CDP-glycerol or FAD) were analyzed by ^{31}P NMR. Protein content was estimated by the Bradford method (24).

NMR spectroscopy. ^{31}P NMR spectra were recorded at 202.45 MHz on a Bruker AVANCEII spectrometer using a 5-mm selective probe head at 25°C. Spectra were acquired with a 60° pulse and a repetition delay of 1.5 s. Proton broadband decoupling was applied during the acquisition time only to avoid heating. Quantification of CDP-glycerol was done using a repetition delay of 15 s, and di-*myo*-inositol phosphate was used as internal standard. Phosphoric acid (85% [vol/vol]) contained in a capillary tube designated at 0 ppm was used as chemical shift reference. L-*myo*-Inositol 1-phosphate, *rac*-glycerol phosphate, and *sn*-glycerol 3-phosphate were quantified by ^{1}H NMR. Spectra were acquired with the same spectrometer operating at 500.13 MHz using a 5-mm inverse detection probe head, with presaturation of the water signal with a repetition delay of 60 s. Formate was used as an internal concentration standard.

SUPPLEMENTAL MATERIAL

Supplemental material for this article may be found at https://doi.org/10.1128/AEM.02462-16.

TEXT S1, PDF file, 0.1 MB.

ACKNOWLEDGMENTS

We thank Sara Rebelo for technical support and Luís Gonçalves for useful discussions.

This work was supported by project LISBOA-01-0145-FEDER-007660 (Microbiologia Molecular, Estrutural e Celular) funded by FEDER through COMPETE2020—Programa Operacional Competitividade e Internacionalização (POCI) and by national funds through Fundação para a Ciência e a Tecnologia (FCT). M.V.R. was awarded a fellowship from FCT (SFRH/BPD/80219/2011). The NMR spectrometers are part of The National NMR Facility, supported by FCT (RECI/BBB-BQB/0230/2012).

REFERENCES

1. Lamosa P, Gonçalves LG, Rodrigues MV, Martins LO, Raven ND, Santos H. 2006. Occurrence of 1-glyceryl-1-*myo*-inosityl phosphate in hyperthermophiles. Appl Environ Microbiol 72:6169–6173. https://doi.org/10.1128/AEM.00852-06.
2. Rodrigues MV. 2011. Heat stress adaptation in hyperthermophiles: biosynthesis of inositol-containing compatible solutes. PhD thesis. Instituto de Tecnologia Química e Biológica, Oeiras, Portugal.
3. Faria TQ, Mingote A, Siopa F, Ventura R, Maycock C, Santos H. 2008. Design of new enzyme stabilizers inspired by glycosides of hyperthermophilic microorganisms. Carbohydr Res 343:3025–3033. https://doi.org/10.1016/j.carres.2008.08.030.
4. Santos H, Lamosa P, Borges N, Gonçalves LG, Pais T, Rodrigues MV. 2010. Organic compatible solutes of prokaryotes that thrive in hot environments: the importance of ionic compounds for thermostablization, p 497–520. *In* Horikoshi K (ed), Extremophiles handbook. Springer Japan, Tokyo, Japan.
5. Faria C, Jorge CD, Borges N, Tenreiro S, Outeiro TF, Santos H. 2013. Inhibition of formation of α-synuclein inclusions by mannosylglycerate in a yeast model of Parkinson's disease. Biochim Biophys Acta 1830:4065–4072. https://doi.org/10.1016/j.bbagen.2013.04.015.
6. Nogly P, Gushchin I, Remeeva A, Esteves AM, Borges N, Ma P, Ishchenko A, Grudinin S, Round E, Moraes I, Borshchevskiy V, Santos H, Gordeliy V, Archer M. 2014. X-ray structure of a CDP-alcohol phosphatidyltransferase membrane enzyme and insights into its catalytic mechanism. Nat Commun 5:4169. https://doi.org/10.1038/ncomms5169.
7. Borges N, Gonçalves LG, Rodrigues MV, Siopa F, Ventura R, Maycock C, Lamosa P, Santos H. 2006. Biosynthetic pathways of inositol and glycerol phosphodiesters used by the hyperthermophile *Archaeoglobus fulgidus* in stress adaptation. J Bacteriol 188:8128–8135. https://doi.org/10.1128/JB.01129-06.
8. Rodrigues MV, Borges N, Henriques M, Lamosa P, Ventura R, Fernandes C, Empadinhas N, Maycock C, da Costa MS, Santos H. 2007. Bifunctional CTP:inositol-1-phosphate cytidylyltransferase/CDP-inositol:inositol-1-phosphate transferase, the key enzyme for di-*myo*-inositol-phosphate synthesis in several (hyper)thermophiles. J Bacteriol 189:5405–5412. https://doi.org/10.1128/JB.00465-07.
9. Brown S, Santa Maria JP, Jr, Walker S. 2013. Wall teichoic acids of Gram-positive bacteria. Annu Rev Microbiol 67:313–336. https://doi.org/10.1146/annurev-micro-092412-155620.
10. Mericl AN, Friesen JA. 2012. Comparative kinetic analysis of glycerol 3-phosphate cytidylyltransferase from *Enterococcus faecalis* and *Listeria monocytogenes*. Med Sci Monit 18:BR427–BR434. https://doi.org/10.12659/MSM.883535.
11. Park YS, Gee P, Sanker S, Schurter EJ, Zuiderweg ER, Kent C. 1997. Identification of functional conserved residues of CTP:glycerol-3-phosphate cytidylyltransferase. Role of histidines in the conserved HXGH in catalysis. J Biol Chem 272:15161–15166.
12. Yim VC, Zolli M, Badurina DS, Rossi L, Brown ED, Berghuis AM. 2001. Crystallization and preliminary X-ray diffraction studies of glycerol 3-phosphate cytidylyltransferase from *Staphylococcus aureus*. Acta Crystallogr D Biol Crystallogr 57:918–920. https://doi.org/10.1107/S0907444901005212.
13. Badurina DS, Zolli-Juran M, Brown ED. 2003. CTP:glycerol 3-phosphate cytidylyltransferase (TarD) from *Staphylococcus aureus* catalyzes the cytidylyl transfer via an ordered Bi-Bi reaction mechanism with micromolar K(m) values. Biochim Biophys Acta 1646:196–206. https://doi.org/10.1016/S1570-9639(03)00019-0.
14. Fong DH, Yim VC, D'Elia MA, Brown ED, Berghuis AM. 2006. Crystal structure of CTP:glycerol-3-phosphate cytidylyltransferase from *Staphylococcus aureus*: examination of structural basis for kinetic mechanism. Biochim Biophys Acta 1764:63–69. https://doi.org/10.1016/j.bbapap.2005.10.015.
15. Weber CH, Park YS, Sanker S, Kent C, Ludwig ML. 1999. A prototypical cytidylyltransferase: CTP:glycerol-3-phosphate cytidylyltransferase from *Bacillus subtilis*. Structure 7:1113–1124. https://doi.org/10.1016/S0969-2126(99)80178-6.
16. Sanker S, Campbell HA, Kent C. 2001. Negative cooperativity of substrate binding but not enzyme activity in wild-type and mutant forms of CTP:glycerol-3-phosphate cytidylyltransferase. J Biol Chem 276:37922–37928.
17. Pattridge KA, Weber CH, Friesen JA, Sanker S, Kent C, Ludwig ML. 2003. Glycerol-3-phosphate cytidylyltransferase. Structural changes induced by binding of CDP-glycerol and the role of lysine residues in catalysis. J Biol Chem 278:51863–51871.
18. Huerta C, Borek D, Machius M, Grishin NV, Zhang H. 2009. Structure and mechanism of a eukaryotic FMN adenylyltransferase. J Mol Biol 389:388–400. https://doi.org/10.1016/j.jmb.2009.04.022.
19. Krupa A, Sandhya K, Srinivasan N, Jonnalagadda S. 2003. A conserved domain in prokaryotic bifunctional FAD synthetases can potentially catalyze nucleotide transfer. Trends Biochem Sci 28:9–12. https://doi.org/10.1016/S0968-0004(02)00009-9.
20. Park YS, Sweitzer TD, Dixon JE, Kent C. 1993. Expression, purification, and characterization of CTP:glycerol-3-phosphate cytidylyltransferase from *Bacillus subtilis*. J Biol Chem 268:16648–16654.
21. Stevens SY, Sanker S, Kent C, Zuiderweg ER. 2001. Delineation of the allosteric mechanism of a cytidylyltransferase exhibiting negative cooperativity. Nat Struct Biol 8:947–952. https://doi.org/10.1038/nsb1101-947.
22. Daiyasu H, Hiroike T, Koga Y, Toh H. 2002. Analysis of membrane stereochemistry with homology modeling of *sn*-glycerol-1-phosphate dehydrogenase. Protein Eng 15:987–995. https://doi.org/10.1093/protein/15.12.987.
23. Koga Y. 2014. From promiscuity to the lipid divide: on the evolution of distinct membranes in Archaea and Bacteria. J Mol Evol 78:234–242. https://doi.org/10.1007/s00239-014-9613-4.
24. Bradford MM. 1976. A rapid and sensitive method for the quantitation of microgram quantities of protein utilizing the principle of protein-dye binding. Anal Biochem 72:248–254. https://doi.org/10.1016/0003-2697(76)90527-3.
25. Sambrook J, Fritsch EF, Maniatis T. 1989. Molecular cloning: a laboratory manual. Cold Spring Harbor Laboratory Press, Cold Spring Harbor, NY.
26. IUPAC-IUB Commission on Biochemical Nomenclature. 1967. The nomenclature of lipids. J Lipid Res 8:523–528.
27. Mashhadi Z, Xu H, Grochowski LL, White RH. 2010. Archaeal RibL: a new FAD synthetase that is air sensitive. Biochemistry 49:8748–8755. https://doi.org/10.1021/bi100817q.
28. Tamura K, Stecher G, Peterson D, Filipski A, Kumar S. 2013. MEGA6: Molecular Evolutionary Genetics Analysis version 6.0. Mol Biol Evol 30:2725–2729. https://doi.org/10.1093/molbev/mst197.